Time-Splitting Chebyshev-Spectral Method for the Schrödinger Equation in the Semiclassical Regime with Zero Far-Field Boundary Conditions

Hongsheng Wang[a], Yushan Ni[a,*] and Junwan Li[b]

[a]*Department of Mechanics and Engineering Science, Fudan University, Shanghai 200433, China*

[b]*School of Materials Science and Engineering, Shanghai University, Shanghai 200072, China*

Abstract: Semiclassical limit of Schrödinger equation with zero far-field boundary conditions is investigated by the time-splitting Chebyshev-spectral method. The numerical results of the position density and current density are presented. The time-splitting Chebyshev-spectral method is based on Strang splitting method in time coupled with Chebyshev-spectral approximation in space. Compared with the time-splitting Fourier-spectral method, the time-splitting Chebyshev-spectral method is unnecessary to treat the wave function as periodic and holds the smoothness of the wave function. For different initial conditions and potential (e.g. constant potential and harmonic potential), extensive numerical test examples in one-dimension are studied. The numerical results are in good agreement with the weak limit solutions. It shows that the time-splitting Chebyshev-spectral method is effective in capturing ε-oscillatory solutions of the Schrödinger equation with zero far-field boundary conditions. In addition, the time-splitting Chebyshev-spectral method surpasses the traditional finite difference method in the meshing strategy due to the exponentially high-order accuracy of Chebyshev-spectral method.

Keywords: Schrödinger equation, time-splitting Chebyshev-spectral method, zero far-field boundary conditions, semiclassical limit.

1. INTRODUCTION

Many problems of solid state physics require the (numerical) solution of the following Schrödinger equation [1-3] in the case of a small Planck constant ε ($0<\varepsilon<<1$):

$$i\varepsilon u_t^\varepsilon = -\frac{\varepsilon^2}{2}\Delta u^\varepsilon + V(x)u^\varepsilon \quad t>0, \quad x\in R^d \tag{1}$$

$$u^\varepsilon(x,t=0) = u_0^\varepsilon(x) \quad x\in R^d \tag{2}$$

where $V(x)$ is a given real-valued electrostatic potential, and $u^\varepsilon = u^\varepsilon(x, t)$ is the complex-valued wave function which is used to compute observables (including the primary physical quantities) in classical quantum physics. The introduction of the small Planck constant ε in Schrödinger equation with oscillatory initial data offers great help for the equation resolution [4]. The work about the behavior of solutions of the nonlinear Schrödinger equation in the semiclassical limit ($\varepsilon\to 0$) was entirely motivated by a natural mathematical question [5], however, in the recent years many researches show that the semiclassical limit of Schrödinger equation is also of direct importance to basic physics and technology in nonlinear optics [5-7]. As mentioned in [5], the semiclassical limit of nonlinear Schrödinger equation provides an idealized description of optical shocks and wave breaking in the nonlinear propagation of laser pulses in optical fibers. In [6, 7], the semiclassical limit of nonlinear Schrödinger equation has also been applied to describe "nonreturn to zero" optical pulses in nonlinear fibers, a problem of central importance of the current technology of long distance (transoceanic) telephone communication. Investigations on the semiclassical limit of Schrödinger equation including theoretical analysis, numerical calculation and application have become an important subject, particularly by the introduction of tools from microlocal analysis, such as defect measures [8], H-measures [9] and Wigner measures [10-12]. These studies have provided technical tools for exploiting properties of Schrödinger equation in the semiclassical regime.

It is well known that Eq. (1) propagates oscillations of wave length $O(\varepsilon)$ in space and time, which inhibit u^ε from converging strongly. This implies that the analysis of the so-called semiclassical limit ($\varepsilon\to 0$) is a mathematically rather complex issue [1, 2, 13], and up to now there has not been a rigorous analytical theory of the semicalssical limit of Schrödinger equation [13], thus it is natural these days to study this problem numerically. Unfortunately, the highly oscillatory nature of the solutions of Schrödinger equation with small ε provides severe numerical burdens [2, 13, 14]. The semiclassical initial value problem, namely Eq. (1) and (2), is a classic example of a "stiff" problem, as it contains two vastly different spatial and temporal scales and involves essential competition between effects on these two scales [13]. Even for stable discretization schemes (or under mesh size restrictions which guarantee stability), the oscillations may very

*Address corresponding to this author at the Department of Mechanics and Engineering Science, Fudan University, Shanghai 200433, China; Tel: +86-21-65642745; Fax: +86-21-65642745; E-mail: niyushan@fudan.edu.cn

PACS numbers: 02.60.Cb, 02.60.Lj, 02.70.Hm, 03.65.Sq.

well disturb the solution in such a way that the quadratic macroscopic quantities and other physical observables come out completely wrong unless the spatial-temporal oscillations are fully resolved numerically, i.e. using many grid points per wavelength of $O(\varepsilon)$ [1, 2]. Markowich [1, 15] *et al.* applied Wigner-transform techniques to the analysis of finite difference methods for Schrödinger equation with small ε and zero far-field boundary conditions ($|u^{\varepsilon}(x,t)|$ decays to zero sufficiently fast as $|x| \to \infty$ [1, 2, 5]), they obtained sharp conditions on the spatial-temporal grid which guaranteed convergence for values of all observables as Plank constant ε tended to zero. Their results show that, for the best combination of the time and space discretizations, one needs the following constraint: mesh size $h = o(\varepsilon)$ and time step $k = o(\varepsilon)$. Failure to satisfy this constraint leads to wrong numerical observables. It appears clearly that the finite difference methods for this problem have very high requirement in the meshing strategy when ε inclines to zero. Since the solution of Schrödinger equation in the semiclassical regime is highly oscillatory but smooth, spectral method is perfect to compute the spatial derivatives of u^{ε} to high accuracy on a simple domain [16], and is helpful to solve the Schrödinger equation in the semiclassical regime. Feit [17] *et al.* used spectral method to determine the eigenvalues and eigenfunctions of Schrödinger equation. Pathria [18] *et al.* studied the time-splitting spectral discretizations of Schrödinger equation for $\varepsilon = O(1)$ which did not give any clue about the semiclassical limit. Recently, Bao *et al.* systemically investigated the time-splitting Fourier -spectral method [2, 19] and time-splitting sine-spectral method [20] for the semiclassical limit of Schrödinger equation with zero far-field boundary conditions and applied them successfully to simulate Bose-Einstein condensation [21]. Bao [22] also proposed the time-splitting Chebyshev-spectral method to preliminarily solve Schrödinger equation with nonzero far-field conditions. Moreover, Zhang [14, 23] *et al.* presented a time-splitting and space-time adaptive wavelet scheme to solve Schrödinger equation with zero far-field boundary conditions.

As a rule, Fourier-spectral method is used to compute the spatial derivatives of the periodic function [16]. For the mathematically nonperiodic function, if it is very close to zero (for example, exponentially decaying to zero) at the ends of the computing interval, one approach would be to regard the function as periodic and to use Fourier-spectral method approximately after choosing an appropriately large computing interval [16]. Based on this approach, although the solution of Schrödinger equation in the semiclassical regime is nonperiodic, Bao [2, 19] presented the time-splitting Fourier-spectral method to solve Schrödinger equation with zero far-field boundary conditions. However, this kind of approximation on periodicity usually damages the smoothness of the wave function, and sacrifices the accuracy advantages of the spectral methods because the accuracy of spectral methods depends on the smoothness of the functions being solved. Sometimes Gibbs phenomenon even occurs [16]. Now that the solution of Schrödinger equation with zero far-field boundary conditions is nonperiodic, it is a better choice to use the time-splitting Chebyshev-spectral method which is more applicable to the nonperiodic function [16].

In this paper, we derive the algorithmic formula of the time-splitting Chebyshev-spectral method and use it to solve Schrödinger equation with zero far-field boundary conditions which is previously solved by the time-splitting Fourier-spectral method [2, 19]. Extensive numerical test examples in one-dimension are studied for different initial conditions and potential (e.g. constant potential and harmonic potential). Comparisons between the numerical results and the weak limits verify the availability of the time-splitting Chebyshev-spectral method for Schrödinger equation with zero far-field boundary conditions. We also present the meshing strategy of the time-splitting Chebyshev-spectral method, and it surpasses the traditional finite difference method due to the exponentially high-order accuracy of Chebyshev-spectral method.

2. TIME-SPLITTING CHEBYSHEV-SPECTRAL METHOD

In this section, we derive the algorithmic formula of the time-splitting Chebyshev -spectral method. We consider Eq. (1) and (2) with zero far-field boundary conditions in the case of one-dimension ($d = 1$):

$$i\varepsilon u_t^{\varepsilon} = -\frac{\varepsilon^2}{2} u_{xx}^{\varepsilon} + V(x)u^{\varepsilon} \quad a < x < b, \quad t > 0 \tag{3}$$

$$u^{\varepsilon}(x, t=0) = u_0^{\varepsilon}(x) \quad a \le x \le b \tag{4}$$

$$u^{\varepsilon}(a,t) = 0 \quad u^{\varepsilon}(b,t) = 0 \quad t \ge 0 \tag{5}$$

It must be pointed out that the solution of Schrödinger equation (3) with zero far-field boundary conditions (5) is nonperiodic. Compared with the time-splitting Fourier-spectral method, we use time-splitting Chebyshev-spectral method to solve this nonperiodic problem.

By classical quantum physics [24] the wave function u^{ε} is an auxiliary quantity used to compute the primary physical quantities, which are quadratic functions of u^{ε}, e.g. the position density

$$\rho^{\varepsilon}(x,t) = |u^{\varepsilon}(x,t)|^2 \tag{6}$$

and the current density

$$J^{\varepsilon}(x,t) = \varepsilon \mathrm{Im}(\overline{u^{\varepsilon}(x,t)} \nabla u^{\varepsilon}(x,t)) \tag{7}$$

where "$\overline{\ }$" denotes complex conjugation.

2.1. Grid Partitioning

For simplicity, we choose the spatial grid points as Chebyshev-Gauss-Lobatto interpolation points [25, 26], then let the grid points be

$$x_j := \frac{b-a}{2}\cos\frac{j\pi}{M} + \frac{b+a}{2} \qquad j = 0,1,....., M \tag{8}$$

We choose the time step size k and let time steps be $t_n := nk \qquad n = 0,1,2,.....$

2.2. Strang Splitting Method

As preparatory steps, we begin by introducing the splitting method [27] for a general evolution equation

$$i\partial_t u = f(u) = Au + Bu \tag{9}$$

where $f(u)$ is a operator and the splitting $f(u) = Au + Bu$ can be quite arbitrary. For a given time step k, let $t_n = nk$, n = 0,1,2, … and u^n be the approximation of $u(t_n)$. Also known as the symmetric operator splitting, a standard second-order Strang splitting method [28-32] in time is as follows:

$$\begin{aligned} u^{*} &= e^{-ikA/2}u^{n} \\ u^{**} &= e^{-ikB}u^{*} \\ u^{n+1} &= e^{-ikA/2}u^{**} \end{aligned} \tag{10}$$

then we can obtain u^{n+1} from u^n by solving Eq. (10).

Eq. (3) multiplying by 1/ε, we get

$$iu_t^{\varepsilon} = -\frac{\varepsilon}{2}u_{xx}^{\varepsilon} + \frac{V(x)}{\varepsilon}u^{\varepsilon} \tag{11}$$

Comparing Eq. (11) with Eq. (9), let

$$Au^{\varepsilon} = \frac{V(x)}{\varepsilon}u^{\varepsilon} \quad Bu^{\varepsilon} = -\frac{\varepsilon}{2}u_{xx}^{\varepsilon} \tag{12}$$

then from time $t = t_n$ to time $t = t_{n+1}$ Eq. (11) can be solved by the following three steps *via* Strang splitting method , namely Eq. (10).

First, we solve

$$i\varepsilon u_t^{\varepsilon} = V(x)u^{\varepsilon} \tag{13}$$

for half of one time step (of length k), followed by solving

$$i\varepsilon u_t^{\varepsilon} = -\frac{\varepsilon^2}{2}u_{xx}^{\varepsilon} \tag{14}$$

with the boundary condition (5) for one time step k.

Finally, we solve

$$i\varepsilon u_t^{\varepsilon} = V(x)u^{\varepsilon} \tag{15}$$

for half of one time step again.

Note that the ODE (13), (15) can be solved exactly:

$$u^{\varepsilon}(x,t) = e^{-iV(x)(t-t_n)/\varepsilon} \cdot u^{\varepsilon}(x,t_n) \quad t \in [t_n, t_{n+1}] \tag{16}$$

therefore we only need to solve Eq. (14) subject to the boundary condition (5).

2.3. Chebyshev-Spectral Method

Eq. (14) with the boundary condition (5) can be discretized in space by Chebyshev-spectral method [25, 26] and integrated in time exactly by applying a diagonalization technique for the ODE system in phase space.

Using Chebyshev interpolation [25, 26], let

$$u_M^{\varepsilon}(x,t) = \sum_{m=0}^{M} a_m(t)T_m\left(\frac{x-(b+a)/2}{(b-a)/2}\right) \quad a \le x \le b \tag{17}$$

where $T_m(x)$ is the m-th Chebyshev polynomial.

$$T_m(x) = \cos(m \arccos x) \tag{18}$$

Plugging the expansion (17) into the boundary condition (5), we have

$$u^{\varepsilon}(a,t) = \sum_{m=0}^{M} a_m(t)T_m(-1) = \sum_{m=0}^{M}(-1)^m a_m(t) = 0 \tag{19}$$

$$u^{\varepsilon}(b,t) = \sum_{m=0}^{M} a_m(t)T_m(1) = \sum_{m=0}^{M} a_m(t) = 0 \tag{20}$$

simplifying as

$$\sum_{\substack{m=0 \\ m \text{ even}}}^{M} a_m = 0 \quad \sum_{\substack{m=1 \\ m \text{ odd}}}^{M} a_m = 0 \tag{21}$$

Plugging the expansion (17) into Eq. (14), we can obtain the following ODE system by using the property of the expansion coefficients of Chebyshev interpolation [25]:

$$i\varepsilon a_m^{'}(t)+\frac{2\varepsilon^2}{(b-a)^2 c_m}\sum_{\substack{p=m+2\\ p+m\ even}}^{M} p(p^2-m^2)a_p(t)=0 \qquad (22)$$

$0 \le m \le M-2$

where $c_0 = 2$, $c_m = 1$ (m>0).

Removing all $a_{M-1}(t)$ and $a_M(t)$ in Eq. (22) by employing Eq. (21), let

$$\vec{a}(t)=\begin{bmatrix} a_0(t)\\ a_1(t)\\ a_2(t)\\ \vdots\\ a_{M-2}(t)\end{bmatrix} \qquad (23)$$

thus the ODE system (22) can now be written as

$$\frac{d\vec{a}(t)}{dt}=\frac{2i\varepsilon}{(b-a)^2}T\vec{a}(t) \qquad (24)$$

where $T = (t_{jk})$ is an $(M-1)\times(M-1)$ constant matrix with entries:

$$t_{jk}=\frac{1}{c_j}\begin{cases} -M(M^2-j^2) & 0\le k\le j \quad j,k\ even\\ k(k^2-j^2)-M(M^2-j^2) & j+2\le k\le M-2 \quad j,k\ even\\ -(M-1)((M-1)^2-j^2) & 1\le k\le j \quad j,k\ odd\\ k(k^2-j^2)-(M-1)((M-1)^2-j^2) & j+2\le k\le M-2 \quad j,k\ odd\\ 0 & else\end{cases} \qquad (25)$$

$$j,k=0,1,2,.....,M-2$$

2.4. Solving *via* Diagonalization Technique

The matrix T has $M-1$ distinct negative eigenvalues [25], therefore it is diagonalizable, i.e. there exists an invertible matrix P and a diagonal matrix D such that

$$T = PDP^{-1} \qquad (26)$$

Let

$$\vec{b}(t)=P^{-1}\vec{a}(t) \qquad (27)$$

Eq. (24) multiplying by the matrix P^{-1}, we obtain

$$\frac{d\vec{b}(t)}{dt}=\frac{2i\varepsilon}{(b-a)^2}D\vec{b}(t) \qquad (28)$$

Since the matrix D is diagonal, the equations in ODE system (28) are actually independent of each other. After a simple calculation, we can get

$$\vec{b}(t)=\exp(\frac{2i\varepsilon(t-t_n)}{(b-a)^2}D)\vec{c} \quad t\in[t_n,t_{n+1}] \qquad (29)$$

where $\vec{c}$ is a vector to be determined.

Combining Eq. (27) and Eq. (29), we have

$$\vec{a}(t)=P\vec{b}(t)=P\exp(\frac{2i\varepsilon(t-t_n)}{(b-a)^2}D)\vec{c} \qquad (30)$$

Choosing $t = t_n$ in Eq. (30), we obtain

$$\vec{a}(t_n)=P\vec{c} \qquad (31)$$

then

$$\vec{c}=P^{-1}\vec{a}(t_n) \qquad (32)$$

Substituting Eq. (32) into Eq. (30), we get

$$\vec{a}(t)=P\exp(\frac{2i\varepsilon(t-t_n)}{(b-a)^2}D)P^{-1}\vec{a}(t_n) \quad t\in[t_n,t_{n+1}] \qquad (33)$$

This implies that we can get $\vec{a}(t_{n+1})$ from $\vec{a}(t_n)$ via Eq. (33).

2.5. Algorithmic Formula

Finally, we state the result for the algorithmic formula of the time-splitting Chebyshev -spectral method.

Let $U_j^{\varepsilon,n}$ be the numerical approximation of $u^{\varepsilon}(x_j, t_n)$ and $U^{\varepsilon,n}$ be the solution vector at time $t = t_n = nk$ with components $U_j^{\varepsilon,n}$.

From time $t = t_n$ to $t = t_{n+1}$, we combine Eq. (16), (17), (21) and (33) *via* the standard second-order Strang splitting and obtain the time-splitting Chebyshev-spectral method. The steps for obtaining $U_j^{\varepsilon,n+1}$ from $U_j^{\varepsilon,n}$ are given by:

1. Solving Eq. (13) for half of one time step

$$U_j^{\varepsilon,*}=e^{-iV(x_j)k/2\varepsilon}U_j^{\varepsilon,n} \quad 0\le j\le M \qquad (34)$$

2. Utilizing Chebyshev transform [26]

$$a_l^{\varepsilon,*}=\frac{1}{\gamma_l}\sum_{m=0}^{M}U_m^{\varepsilon,*}\omega_m T_l(\frac{x_m-(b+a)/2}{(b-a)/2}) \quad 0\le l\le M \qquad (35)$$

where

$$w_0=w_M=\frac{\pi}{2M} \quad w_m=\frac{\pi}{M}\ (1\le m\le M-1)$$
$$\gamma_0=\gamma_M=\pi \quad \gamma_m=\frac{\pi}{2}\ (1\le m\le M-1) \qquad (36)$$

3. According to Eq. (33), we obtain

$$\vec{a}^{\varepsilon,**} = P\exp(\frac{2i\varepsilon k}{(b-a)^2}D)P^{-1}\vec{a}^{\varepsilon,*} \tag{37}$$

for one time step k.

4. Based on Eq. (21), we get

$$a_{M-1}^{\varepsilon,**} = -\sum_{\substack{m=1\\ m \text{ odd}}}^{M-2} a_m^{\varepsilon,**} \qquad a_M^{\varepsilon,**} = -\sum_{\substack{m=0\\ m \text{ even}}}^{M-2} a_m^{\varepsilon,**} \tag{38}$$

5. According to Eq. (17), we have

$$U_j^{\varepsilon,**} = \sum_{m=0}^{M} a_m^{\varepsilon,**} T_m(\frac{x_j-(b+a)/2}{(b-a)/2}) \qquad 0 \le j \le M \tag{39}$$

6. Solving Eq. (15) for half of one time step again

$$U_j^{\varepsilon,n+1} = e^{-iV(x_j)k/2\varepsilon}U_j^{\varepsilon,**} \qquad 0 \le j \le M \tag{40}$$

In the above progress, we used the second-order Strang splitting method. For different precision requirement, we could choose other high-order splitting methods [33].

3. EXAMPLES AND NUMERICAL RESULTS

In this section, for different initial conditions and potential, we study numerically the meshing strategy of time-splitting Chebyshev-spectral method for Schrödinger equation with zero far-field boundary conditions and investigate the semiclassical limit ($\varepsilon \to 0$) of Schrödinger equation in one-dimension.

In our computations, the initial condition is always chosen in the classical WKB form:

$$u^{\varepsilon}(x,t=0) = u_0^{\varepsilon}(x) = A_0(x)e^{iS_0(x)/\varepsilon} = \sqrt{\rho_0(x)}e^{iS_0(x)/\varepsilon} \tag{41}$$

with A_0 and S_0 independent of ε, real valued and with $A_0(x)$ decaying to zero sufficiently fast as $|x| \to \infty$. We remark that the initial condition (41) is oscillatory, and Schrödinger equation (3) propagates oscillations of wave length $O(\varepsilon)$ in space and time.

We choose an appropriately long interval [a, b] for the computations such that the zero far-field boundary conditions (5) do not introduce a significant error relative to the whole space problem.

As already pointed out, the main goal when solving Schrödinger equation is to compute macroscopic quantities (e.g. the position density and the current density) associated to the wave function, in the following computations we therefore give the numerical results of the position density $\rho^{\varepsilon}(x, t)$ and the current density $J^{\varepsilon}(x, t)$ rather than the results of wave function $u^{\varepsilon}(x, t)$.

Two sets of numerical experiments are designed in the following.

Example 1 (Markowich, Pietra and Pohl [1, 15])

The initial condition is taken as

$$\rho_0(x) = (e^{-25(x-0.5)^2})^2 \qquad S_0(x) = 0.2(x^2 - x) \tag{42}$$

We solve on the x-interval [0, 1], i.e. $a = 0$ and $b = 1$. Let $V(x) = 100$ be a constant potential.

In order to test the meshing strategy of the time-splitting Chebyshev-spectral method and to investigate the semiclassical limit ($\varepsilon \to 0$), we compute the following three cases with different combinations of ε and M

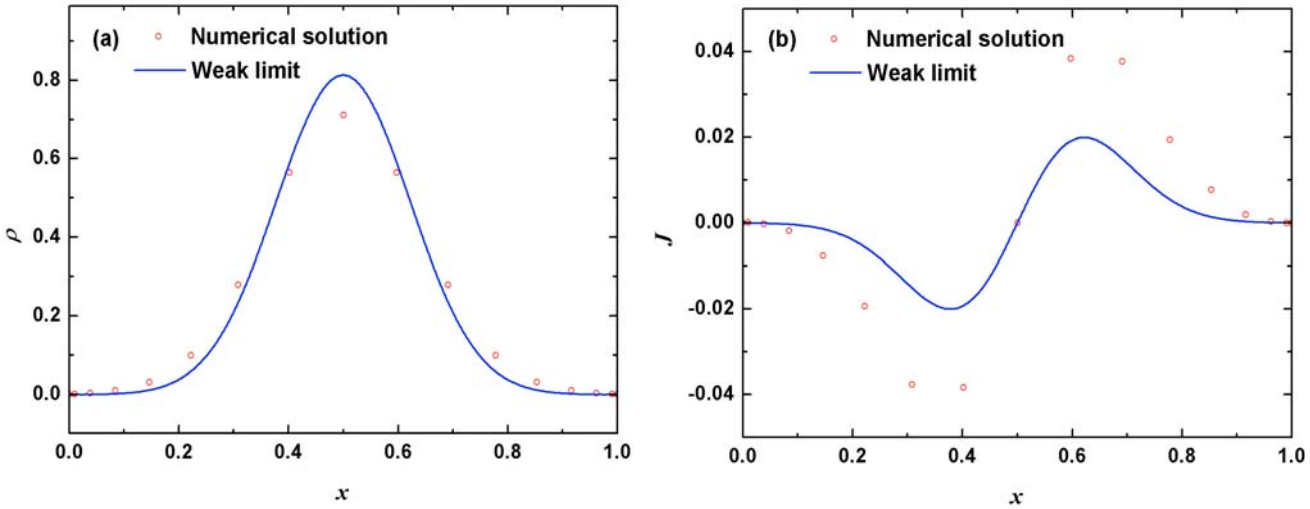

Figure 1: (**a**) position density and (**b**) current density at $t_1 = 0.54$, $\varepsilon_1 = 0.0256$, $M_1 = 16$, $k_1 = 0.03$.

Case (I): $(t_1, \varepsilon_1, M_1, k_1) = (0.54,\ 0.0256,\ 16,\ 0.03)$

Case (II): $(t_2, \varepsilon_2, M_2, k_2) = (0.54,\ 0.0064,\ 64,\ 0.03)$

Case (III): $(t_3, \varepsilon_3, M_3, k_3) = (0.54,\ 0.0008,\ 512,\ 0.03)$

They are all under the meshing strategy: $\frac{b-a}{M} = O(\varepsilon)$, $k = O(\varepsilon)$. The results are displayed in Figures **1**, **2** and **3**, respectively.

The weak limits $\rho^0(x, t)$, $J^0(x, t)$ of $\rho^\varepsilon(x, t)$, $J^\varepsilon(x, t)$, respectively, as $\varepsilon \to 0$, have been given in [1, 2, 15]. As a reference purposes, we also plot them at $t = 0.54$ in Figures **1**, **2** and **3**.

In case (I), as shown in Figure **1**, $\varepsilon_1 = 0.0256$ is too large compared to zero, and the error between numerical results and weak limits is large.

In case (II), we perform tests similar to those in case (I). Figure **2** shows the corresponding results. Due to $\varepsilon_2 = 0.0064$ close to zero, the error between numerical results and weak limits is much smaller than the error in Figure **1**.

In case (III), $\varepsilon_3 = 0.0008$ is sufficiently small, thus the numerical solutions capture the correct weak limits in Figure **3**.

Although the macroscopic quantities $\rho^\varepsilon(x, 0.54)$ and $J^\varepsilon(x, 0.54)$ for the initial condition (42) have no oscillations in Figure **1**, **2** and **3**, respectively, the wave function u^ε has oscillations in the phase [1]. A choice of the discretization parameters that does not take care of the oscillations can give the wrong results [1]. As far as this example is concerned, in order to guarantee good approximations for ε small, the traditional finite difference method needs the following constraint [1]: $h = o(\varepsilon)$, $k = o(\varepsilon)$. However, in Figure **1**, **2** and **3**, we can observe numerical convergence (in the weak sense) to

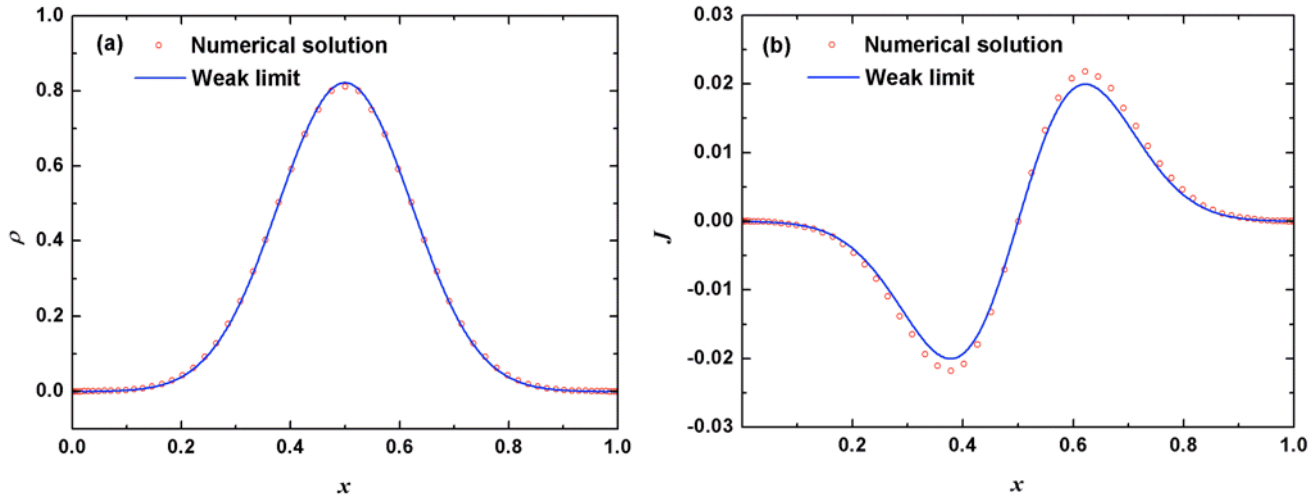

Figure 2: (**a**) position density and (**b**) current density at $t_2 = 0.54$, $\varepsilon_2 = 0.0064$, $M_2 = 64$, $k_2 = 0.03$.

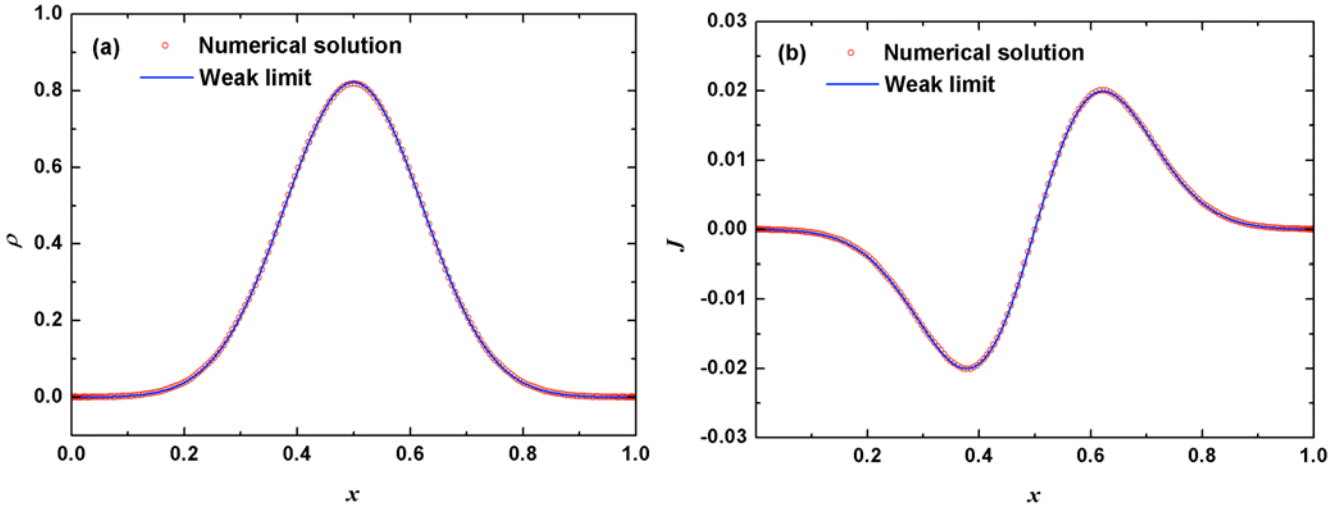

Figure 3: (**a**) position density and (**b**) current density at $t_3 = 0.54$, $\varepsilon_3 = 0.0008$, $M_3 = 512$, $k_3 = 0.03$.

the limit solution as $\varepsilon \to 0$ under the meshing strategy "$\frac{b-a}{M} = O(\varepsilon)$, $k = O(\varepsilon)$". This shows that the time-splitting Chebyshev-spectral method has much better resolution for oscillatory solutions of Schrödinger equation than the finite difference method.

Example 2 (Gasser, Markowich [10])

The initial condition is taken as

$$\rho_0(x) = (e^{-25(x-0.5)^2})^2 \qquad S_0(x) = x + 1 \tag{43}$$

We solve on the x-interval [-2, 2], i.e. $a = -2$ and $b = 2$. Let $V(x) = x^2/2$, which is a harmonic oscillator.

Once more, in order to test the meshing strategy of the time-splitting Chebyshev-spectral method and to investigate the semiclassical limit ($\varepsilon \to 0$), we compute the following two cases with different combinations of ε and M

Case (I): $(t_1, \varepsilon_1, M_1, k_1) = (0.52, 0.0025, 1024, 0.02)$

Case (II): $(t_2, \varepsilon_2, M_2, k_2) = (3.6, 0.0025, 1024, 0.02)$

They are all under the meshing strategy: $\frac{b-a}{M} = O(\varepsilon)$, $k = O(\varepsilon)$. The results are displayed in Figures **4** and **5**, respectively.

The weak limits $\rho^0(x, t)$, $J^0(x, t)$ of $\rho^\varepsilon(x, t)$, $J^\varepsilon(x, t)$, respectively, as $\varepsilon \to 0$, have been given in [2, 10]. As a reference purposes, we also plot them at $t_1 = 0.52$ in Figure **4** and $t_2 = 3.6$ in Figure **5**, respectively.

To obtain a better visualization in Figures **4** and **5**, we depict the solutions in a subinterval instead of in the whole computational interval [-2, 2]. In Figures **4** and **5**, we can see numerical convergence to the weak limits for different t with $\varepsilon = 0.0025$ which is very close to zero.

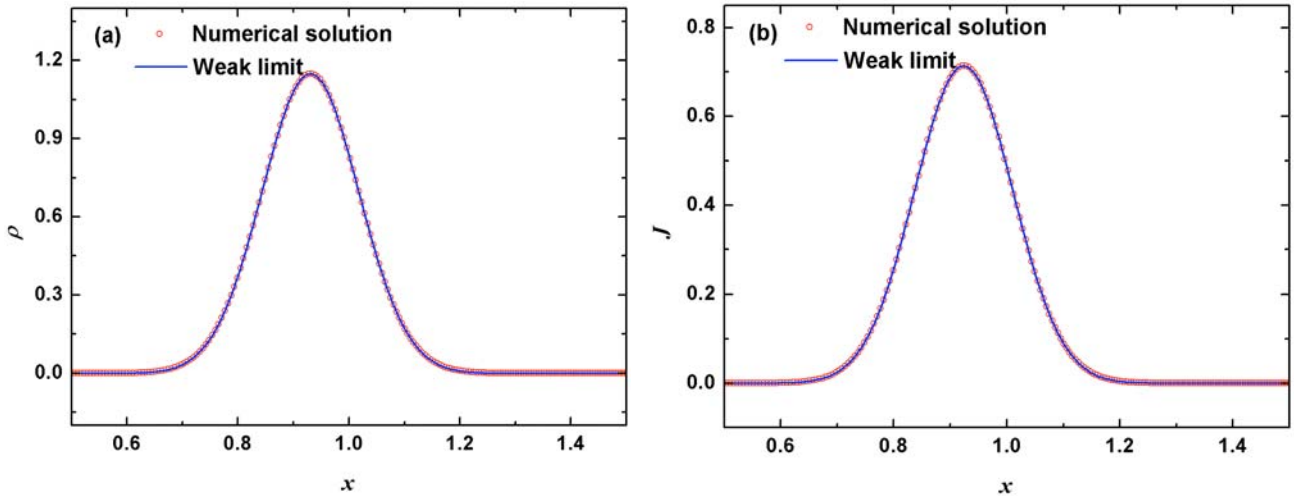

Figure 4: (**a**) position density and (**b**) current density at $t_1 = 0.52$, $\varepsilon_1 = 0.0025$, $M_1 = 1024$, $k_1 = 0.02$.

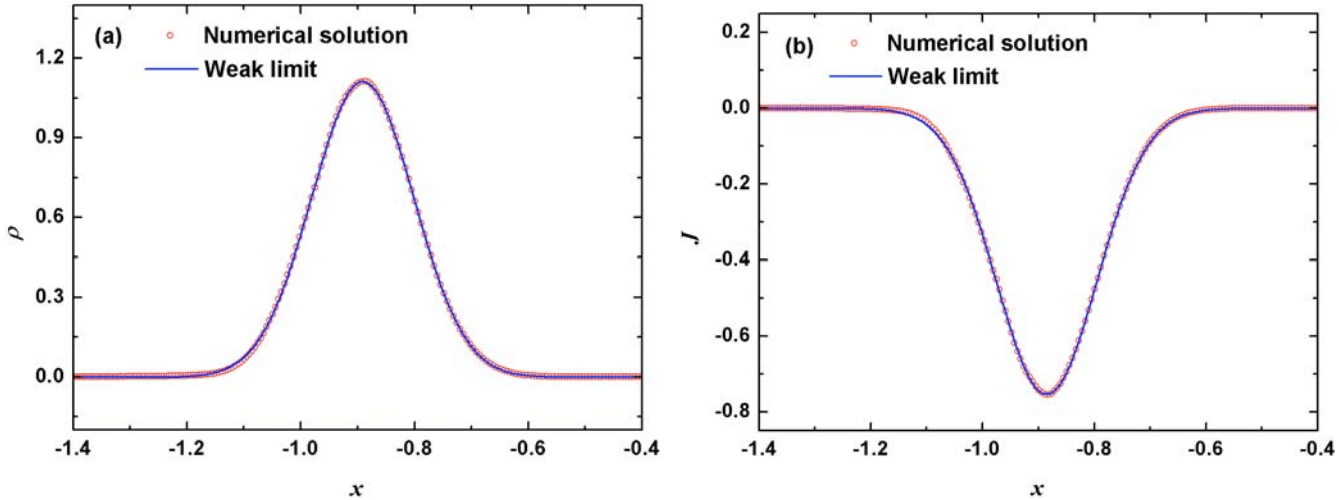

Figure 5: (**a**) position density and (**b**) current density at $t_2 = 3.6$, $\varepsilon_2 = 0.0025$, $M_2 = 1024$, $k_2 = 0.02$.

Remark 1. From the numerical results of these two examples, in which different initial conditions and potential are studied, we can see that the time-splitting Chebyshev-spectral method gives very promising results under the meshing strategy "$\frac{b-a}{M}=O(\varepsilon)$, k = $O(\varepsilon)$" for Schrödinger equation with zero far-field boundary conditions.

4. CONCLUSIONS

Semiclassical limit ($\varepsilon\to 0$) of Schrödinger equation with zero far-field boundary conditions is investigated by the time-splitting Chebyshev-spectral method. The time-splitting Chebyshev-spectral method is based on Strang splitting method in time coupled with Chebyshev-spectral approximation in space. Compared with the time-splitting Fourier-spectral method, the time-splitting Chebyshev-spectral method is unnecessary to treat the wave function as periodic and holds the smoothness of the wave function. It must be pointed out that the solution of Schrödinger equation with zero far-field boundary conditions is nonperiodic and the accuracy of spectral methods depends on the smoothness of the functions being approximated. Therefore, the time-splitting Chebyshev-spectral method can elude the risk of sacrificing the accuracy advantages of the spectral methods and the risk of Gibbs phenomenon. For different initial conditions and potential (e.g. constant potential and harmonic potential), our numerical results capture the correct weak limits as $\varepsilon\to 0$ and show that the time-splitting Chebyshev-spectral method gives promising results for ε small when the meshing strategy satisfies "$\frac{b-a}{M}=O(\varepsilon)$, k = $O(\varepsilon)$", while the frequently used finite difference methods require mesh size and time step much smaller than Plank constant ε. It appears clearly that the time-splitting Chebyshev-spectral method has much better resolution for oscillatory solutions of Schrödinger equation than the finite difference methods. In addition, the application of the diagonalization technique greatly simplifies the calculation process, in which the equations in ODE system are transformed to be independent of each other. Hence, the time-splitting Chebyshev-spectral method is very effective in capturing ε-oscillatory solutions of Schrödinger equation with zero far-field boundary conditions in the semiclassical regime and it is a better choice compared with the time-splitting Fourier-spectral method and the finite difference methods in the case of zero far-field boundary conditions.

ACKNOWLEDGEMENTS

This work was supported by the National Natural Science Foundation of China (Grant No. 10576010). The authors would like to heartfully thank Professor Weizhu Bao of National University of Singapore for his help.

REFERENCES

[1] Markowich PA, Pietra P, Pohl C. Numerical approximation of quadratic observables of Schrödinger-type equations in the semi-classical limit. Numer Math 1999; 81: 595-30. http://dx.doi.org/10.1007/s002110050406

[2] Bao W, Jin S, Markowich PA. On time-splitting spectral approximations for the Schrödinger equation in the semiclassical regime. J Comput Phys 2002; 175: 487-24. http://dx.doi.org/10.1006/jcph.2001.6956

[3] Alonso MA, Forbes GW. New approach to semiclassical analysis in mechanics. J Math Phys 1999; 40: 1699-18. http://dx.doi.org/10.1063/1.532829

[4] Fannjiang A, Jin S, Papanicolaou G. High frequency behavior of the focusing nonlinear Schrödinger equation with random inhomogeneities. SIAM J Appl Math 2003; 63: 1328-58. http://dx.doi.org/10.1137/S003613999935559X

[5] Bronski JC, McLaughlin DW. Semiclassical behavior in the NLS equation: Optical shocks-focusing instabilities. In: Ercolani N M, Gabitov I R, Levermore C D, Serre D, editiors. Singular limits of dispersive waves; 1991: NATO Adv. Sci. Inst. Ser. B Phys., 320. Plenum 1994: pp. 21-38.

[6] Forest MG, McLaughlin KT–R. Onset of oscillations in nonsoliton pulses in nonlinear dispersive fibers. J Nonlinear Sci 1998; 8: 43-62. http://dx.doi.org/10.1007/s003329900043

[7] Kodama Y, Wabnitz S. Analytical theory of guiding-center nonreturn-to-zero and return-to-zero signal transmission in normally dispersive nonlinear optical fibers. Optics Lett 1995; 20: 2291-93. http://dx.doi.org/10.1364/OL.20.002291

[8] Gérard P. Microlocal defect measures. Comm PDE 1991; 16: 1761-94. http://dx.doi.org/10.1080/03605309108820822

[9] Tartar L. H-measures, a New Approach for Studying Homogenization, Oscillations and Concentration Effects in Partial Differential Equations. Proc Roy Soc Edinburgh Sect A 1990; 115: 193-30. http://dx.doi.org/10.1017/S0308210500020606

[10] Gasser I, Markowich PA. Quantum hydrodynamics, Wigner transform and the classical limit. Asymptotic Anal 1997; 14: 97-116.

[11] Gérard P, Markowich PA, Mauser NJ, Poupaud F. Homogeneization limits and Wigner transforms. Comm Pure Appl Math 1997; 50: 323-79. http://dx.doi.org/10.1002/(SICI)1097-0312(199704)50:4<323::AID-CPA4>3.0.CO;2-C

[12] Markowich PA, Mauser NJ, Poupaud F. A Wigner function approach to semiclassical limits: electrons in a periodic potential. J Math Phys 1994; 35: 1066-94. http://dx.doi.org/10.1063/1.530629

[13] Miller PD, Kamvissis S. On the semiclassical limit of the focusing nonlinear Schrödinger equation. Phys Lett A 1998; 247: 75-86. http://dx.doi.org/10.1016/S0375-9601(98)00565-9

[14] Zhang R, Zhang K. Application of time-splitting and wavelet based space-time adaptive method to solving Schrödinger equations. J Jilin Univ 2004; 42: 176-78.

[15] Markowich PA, Pietra P, Pohl C, Stimming HP. A Wigner-measure analysis of the Dufort-Frankel scheme for the Schrödinger equation. SIAM J Numer Anal 2002; 40: 1281-10. http://dx.doi.org/10.1137/S0036142900381734

[16] Trefethen Lloyd N. Spectral Methods in MATLAB: Philadelphia 2000. http://dx.doi.org/10.1137/1.9780898719598

[17] Feit MD, Fleck JA, Steiger A. Solution of the Schrödinger equation by a spectral method. J Comput Phys 1982; 47: 412-33. http://dx.doi.org/10.1016/0021-9991(82)90091-2

[18] Pathria D, Morris JL. Pseudospectral solution of nonlinear Schrödinger equations. J Comput Phys 1990; 87: 108-25. http://dx.doi.org/10.1016/0021-9991(90)90228-S

[19] Bao W, Jin S, Markowich PA. Numerical study of time-splitting spectral discretizations of nonlinear Schrödinger equations in the semi-classical regimes. SIAM J Sci Comput 2003; 25: 27-64. http://dx.doi.org/10.1137/S1064827501393253

[20] Bao W, Jaksch D. An explicit unconditionally stable numerical method for solving damped nonlinear Schrödinger equations with a focusing nonlinearity. SIAM J Numer Anal 2003; 41: 1406-26. http://dx.doi.org/10.1137/S0036142902413391

[21] Bao W, Jaksch D, Markowich PA. Numerical solution of the Gross-Pitaevskii equation for Bose-Einstein condensation. J Comput Phys 2003; 187: 318-42. http://dx.doi.org/10.1016/S0021-9991(03)00102-5

[22] Bao W. Numerical methods for the nonlinear Schrödinger equation with nonzero far-field conditions. Methods Appl Anal 2004; 11: 367-87.

[23] Zhang R, Zhang K, Zhou YS. Numerical study of time-splitting, space-time adaptive wavelet scheme for Schrödinger equations. J Comput Appl Math 2006; 195: 263-73. http://dx.doi.org/10.1016/j.cam.2005.03.086

[24] Landau LD, Lifschitz EM. Lehrbuch der Theoretischen Physik III- Quantenmechanik: Akademic-Verlag 1985.

[25] Gottlieb D, Orszag SA. Numerical Analysis of Spectral methods: Philadelphia 1977.

[26] Canuto C, Hussaini MY, Quarteroni A, Zhang TA. Spectral Methods in Fluid Dynamics: Springer-Verlag 1988.

[27] Fornberg B, Driscoll TA. A fast spectral algorithm for nonlinear wave equations with linear dispersion. J Comput Phys 1999; 155: 456-67. http://dx.doi.org/10.1006/jcph.1999.6351

[28] Strang G. On the construction and composition of difference schemes. SIAM J Numer Anal 1968; 5: 506-17. http://dx.doi.org/10.1137/0705041

[29] Gradinaru V. Strang splitting for the time-dependent Schrödinger equation on sparse grids. SIAM J Numer Anal 2007; 46: 103-23. http://dx.doi.org/10.1137/050629823

[30] Gradinaru V, Tübingen. Fourier transform on sparse grids: code design and application to the time dependent Schrödinger equation. Computing 2007; 80: 1-22. http://dx.doi.org/10.1007/s00607-007-0225-3

[31] Jahnke T, Lubich C. Error bounds for exponential operator splitting. BIT 2000; 40: 735-44. http://dx.doi.org/10.1023/A:1022396519656

[32] Sportisse B. An analysis of operator splitting techniques in the stiff case. J Comput Phys 2000; 161: 140-68. http://dx.doi.org/10.1006/jcph.2000.6495

[33] Yoshida H. Construction of higher order symplectic integrators. Phys Lett A 1990; 150: 262-68. http://dx.doi.org/10.1016/0375-9601(90)90092-3

Received on 31-12-2012 Accepted on 16-01-2013 Published on 01-02-2013

http://dx.doi.org/120.29169/1927-5129.2013.09.11